© 2020. Published by The Company of Biologists Ltd | Journal of Cell Science (2020) 133, jcs243956. doi:10.1242/jcs.243956

SHORT REPORT

Disease-associated keratin mutations reduce traction forces and compromise adhesion and collective migration

Sachiko Fujiwara[1,*,‡], Shinji Deguchi[2] and Thomas M. Magin[1,‡]

ABSTRACT

Keratin intermediate filament (IF) proteins constitute the major cytoskeletal components in epithelial cells. Missense mutations in keratin 5 (K5; also known as KRT5) or keratin 14 (K14; also known as KRT14), highly expressed in the basal epidermis, cause the severe skin blistering disease epidermolysis bullosa simplex (EBS). EBS-associated mutations disrupt keratin networks and change keratinocyte mechanics; however, molecular mechanisms by which mutations shape EBS pathology remain incompletely understood. Here, we demonstrate that, in contrast to keratin-deficient keratinocytes, cells expressing $K14_{R125C}$, a mutation that causes severe EBS, generate lower traction forces, accompanied by immature focal adhesions with an altered cellular distribution. Furthermore, mutant keratinocytes display reduced directionality during collective migration. Notably, RhoA activity is downregulated in human EBS keratinocytes, and Rho activation rescues stiffness-dependent cell–extracellular matrix (ECM) adhesion formation of EBS keratinocytes. Collectively, our results strongly suggest that intact keratin IF networks regulate mechanotransduction through a Rho signaling pathway upstream of cell–ECM adhesion formation and organized cell migration. Our findings provide insights into the underlying pathophysiology of EBS.

This article has an associated First Person interview with the first author of the paper.

KEY WORDS: Epidermolysis bullosa simplex, Intermediate filaments, Keratins, Mechanotransduction, Rho signaling, Traction force

INTRODUCTION

Cells sense and respond to surrounding mechanical cues by activating mechanotransduction pathways, which govern fundamental processes, including development, tissue repair and homeostasis (DuFort et al., 2011; Eyckmans et al., 2011; Evans et al., 2013; Iskratsch et al., 2014; Wang et al., 2015; Hsu et al., 2018). Tensile forces on the actin cytoskeleton and intermediate filaments (IFs) promote formation and maturation of adhesive structures. Adaptation to their mechanical environment requires cells to balance outside and inside forces by exerting appropriate forces against adhesion sites. Basal skin keratinocytes are under tension at the cell–extracellular matrix (ECM) and at cell–cell contact sites, and rely on keratin IFs to provide essential structural support by connecting to the ECM via hemidesmosomes and to neighboring cells via desmosomes (Block et al., 2005; Hatzfeld et al., 2017; Etienne-Manneville, 2018). Mutations in keratin or in desmosomal and hemidesmosomal protein-coding genes cause cell and tissue fragility and compromise mechanical resilience, resulting in skin blistering such as that observed in epidermolysis bullosa simplex (EBS) (Coulombe and Lee, 2012; Homberg and Magin, 2014). Mutation of keratin 14 (K14; also known as KRT14) at residue $K14_{R125}$ (corresponding to the mouse $K14_{R131}$ residue) is the most frequent mutation associated with EBS (www.interfil.org/; Szeverenyi et al., 2008) and causes extensive keratin aggregation and adhesion defects (Homberg et al., 2015; Seltmann et al., 2015). Although these data establish that disrupted keratins cause EBS through compromising mechanical resilience in keratinocytes, the overall contribution of keratins to mechanotransduction remains unclear.

Rho-family GTPases play key roles in actin cytoskeletal reorganization and focal adhesion (FA) formation (Chrzanowska-Wodnicka and Burridge, 1996; Ishizaki et al., 1997; Jaffe and Hall, 2005). In response to mechanical stimuli, increased RhoA activity adapts cells to their mechanical environment. In this setting, keratin 18 (K18; also known as KRT18) mediates tensional force-induced RhoA activation and stress fiber reinforcement (Fujiwara et al., 2016), suggesting that keratins are important regulators of RhoA activity. Changes in local microenvironment, particularly force distribution, may affect keratin-mediated signaling pathways through changing keratin network conformation and/or properties, following posttranslational modifications (Snider and Omary, 2014; Loschke et al., 2015). Moreover, keratins act by scaffolding signaling proteins such as Src, PKC, TRADD, 14-3-3, and Fas receptors (Gilbert et al., 2001; Inada et al., 2001; Kröger et al., 2013; Rotty and Coulombe, 2012; Sanghvi-Shah and Weber, 2017; Mariani et al., 2020).

Here, we investigated the involvement of keratins in mechanotransduction of basal epidermal keratinocytes. We compared mouse keratinocytes stably expressing wild-type (WT) K14 or the $K14_{R131P}$ mutant in cells lacking all type I keratin genes ($KtyI^{-/-}$) (Homberg et al., 2015). We report that intact keratin networks are critical for traction force generation, focal adhesion formation, stiffness-dependent cell adhesion, and directed collective migration. Notably, the EBS-associated $K14_{R125/131}$ mutation significantly reduces RhoA activity, thereby compromising cell adhesion. Moreover, Src–FAK signaling pathways are involved in keratin-mediated signal transduction. Our data provide new insights into the involvement of keratin IFs in cellular mechanotransduction and the pathophysiology of EBS.

[1]Institute of Biology, Faculty of Life Sciences, University of Leipzig, Leipzig 04103, Germany. [2]Division of Bioengineering, Graduate School of Engineering Science, Osaka University, Toyonaka 560-8531, Japan.
*Present address: Graduate School of Biomedical and Health Sciences, Hiroshima University, Hiroshima 734-8553, Japan.

‡Authors for correspondence (sachiko.fujiwara@uni-leipzig.de; t.magin@uni-leipzig.de)

S.F., 0000-0002-5620-637X; T.M.M., 0000-0001-7016-2409

Handling Editor: Kathleen Green
Received 14 January 2020; Accepted 19 June 2020

Journal of Cell Science (2020) 133, jcs243956. doi:10.1242/jcs.243956

RESULTS AND DISCUSSION

The EBS-associated $K14_{R124/131}$ mutation weakens traction forces and downregulates RhoA activity in keratinocytes

We have previously shown that mutation of keratin 14 (K14; also known as KRT14) at residue $K14_{R125}$ decreases keratinocyte stiffness (Homberg et al., 2015). Because cell mechanics is highly related to cellular mechanotransduction, we hypothesized that *KtyI*$^{-/-}$ cells expressing wild-type K14 (K14-WT) and *KtyI*$^{-/-}$ cells expressing $K14_{R131P}$ ($K14_{R131P}$) differ in their ability to generate traction forces. Traction forces were measured using silicone elastomer substrates, which allow visualization and quantification of traction forces following wrinkle formation on substrates (Ichikawa et al., 2017; Fig. 1A,B). Wrinkle length and the percentage of cells forming wrinkles were significantly decreased in $K14_{R131P}$ compared to K14-WT, indicating a lower ability to generate traction forces in the former (Fig. 1C,D). These results suggest that intact keratin networks assume key roles in traction force generation, resulting from mechanotransduction at cell–ECM adhesion sites.

To understand the molecular mechanisms of keratin network-mediated mechanotransduction, we focused on RhoA signaling, which is critical in actomyosin regulation that underlies traction force generation. Examination of active RhoA in $K14_{R131P}$ compared to that in K14-WT revealed significantly lower levels in the former (Fig. 1E). The finding that active RhoA was also strongly diminished in human EBS keratinocytes expressing $K14_{R125C}$ ($K14_{R125C}$) compared to normal human keratinocytes (NHK) (Fig. S2C), suggested that EBS-associated K14 mutations downregulate RhoA activity.

Keratin organization affects cell morphology, actin reorganization, and focal adhesion distribution through RhoA signaling

Traction force generation depends on proper FA formation and actin reorganization. To understand mechanisms underlying reduced traction force generation in $K14_{R131P}$ compared to K14-WT, we analyzed actin and FA organization. We confirmed the expression of K14 and keratin 5 (K5; also known as KRT5) in both cell lines (Fig. S2G). K14-WT are characterized by well-organized keratin networks evenly distributed throughout the cell. By contrast, $K14_{R131P}$ formed extensive aggregates throughout the cytoplasm instead of filaments (Fig. 2A; Fig. S3C; Homberg et al., 2015). Whereas most K14-WT formed pronounced peripheral actin filament bundles, $K14_{R131P}$ possessed actin-rich protrusions, but lacked peripheral actin bundles and showed smaller cell size compared to K14-WT (Fig. 2A–C, Water). Vinculin staining revealed large FAs exclusively at the cell periphery in K14-WT, whereas peripheral FA were significantly reduced in $K14_{R131P}$ (Fig. 2A,D, Water). Careful quantification of the FA area, based on vinculin fluorescence signals (Fig. S4), revealed a decrease in the ratio of FA to cell area in $K14_{R131P}$ compared to K14-WT (Fig. 2E). Immunoblotting confirmed unaltered vinculin levels in both cell lines, indicating that the $K14_{R131P}$ mutation did not affect vinculin levels but suppressed its localization to FAs (Fig. S2H). Immunostaining showed that RhoA localized diffusely throughout the cytoplasm and at the periphery in K14-WT, with some perinuclear enrichment, as previously reported (Kranenburg et al., 1997; Michaelson et al., 2001; Yonemura et al., 2004). By contrast, in $K14_{R131P}$, RhoA was distributed throughout the cytoplasm, but was diminished at the periphery (Fig. S2I). These results suggest that intact keratin networks are important for the localization of RhoA to the cell periphery to promote actin reorganization and peripheral FA formation.

The reduced RhoA activity in human EBS keratinocytes expressing $K14_{R125C}$, compared to NHK (Fig. S2C), raises the question of whether these alterations might be relevant for the pathophysiology of EBS. In agreement with previous results, $K14_{R125C}$ showed aggregated keratins in the cell periphery, in addition to thick perinuclear keratin bundles, whereas NHK displayed an extensive keratin cytoskeleton (Fig. S2A; D'Alessandro et al., 2002; Russell et al., 2004). Based on vinculin staining, the ratio of FA to cell area was significantly lower in $K14_{R125C}$ compared to NHK (Fig. S2B), suggesting that FA formation is downregulated in $K14_{R125C}$. Thus, $K14_{R125C}$ mutations cause similar alterations in EBS keratinocytes and engineered mouse keratinocytes.

Depletion of keratin 6 (K6) in keratinocytes, and of vimentin in fibroblasts and carcinoma cells, reinforces actin cytoskeletal structures and increases cellular traction forces (Wong and Coulombe, 2003; Jiu et al., 2017). Consistent with these reports, *KtyI*$^{-/-}$ keratinocytes showed intense vinculin staining, and the ratio of FA area to cell area was increased compared to wild-type (WT) keratinocytes (Fig. S2D,E). In addition, the activity of RhoA was significantly upregulated in *KtyI*$^{-/-}$ (Fig. S2F). Considering the suppression of FA in $K14_{R131P}$ (Fig. 2A,D), our data demonstrate that absence of keratins and expression of EBS-associated keratin mutants have opposite effects. How disease-associated keratin aggregates disturb the machinery controlling actin reorganization and FA formation requires future studies. The current data establish that intact keratin networks mediate actin reorganization and FA formation.

To examine the significance of RhoA levels in cell adhesion and morphology, we restored endogenous Rho activity using the Rho activator CN03. CN03 treatment increased phosphorylation levels of myosin light chain-2 (Myl2), as shown by immunoblot and immunofluorescence analysis (Fig. 1F,G). CN03 treatment did not significantly affect actin organization or the area and localization of FAs in K14-WT (Fig. 2A,C–E), possibly because Rho activity in these cells is already high in the experimental conditions. However, CN03 treatment increased the ratio of FA area to cell area in $K14_{R131P}$ (Fig. 2E); at the same time, the peripheral distribution of actin bundles and of FAs remained largely unaltered (Fig. 2C,D). This suggests that global activation of Rho, in the presence of aggregated keratins, promotes FA maturation but is insufficient to restore actin reorganization and FA localization. We hypothesize that intact keratin networks contribute to localized RhoA activation in order to regulate actin reorganization and to promote peripheral FA formation.

Aggregation and disorganization of keratin networks by the $K14_{R131P}$ mutation are independent of plectin

The cytolinker protein plectin plays important roles in cytoskeletal network reorganization (Wiche, 1998). For example, plectin mediates the functional interplay between vimentin IFs and actomyosin arcs, and plectin depletion suppresses the dynamics of these two cytoskeletons (Jiu et al., 2015). Because actin structures were different between K14-WT and $K14_{R131P}$, we asked whether $K14_{R131P}$-induced keratin aggregation might mediate actin reorganization via plectin. In both K14-WT and $K14_{R131P}$, plectin was distributed throughout the cytoplasm and remained unaltered in both cell lines transfected with control siRNA (Fig. S3C). Treatment with a targeting siRNA effectively suppressed plectin mRNA and protein expression (Fig. S3A,B); however, it did not affect distribution or size of aggregated keratins in $K14_{R131P}$. While we cannot exclude an involvement of plectin in cell contractility and

Journal of Cell Science (2020) 133, jcs243956. doi:10.1242/jcs.243956

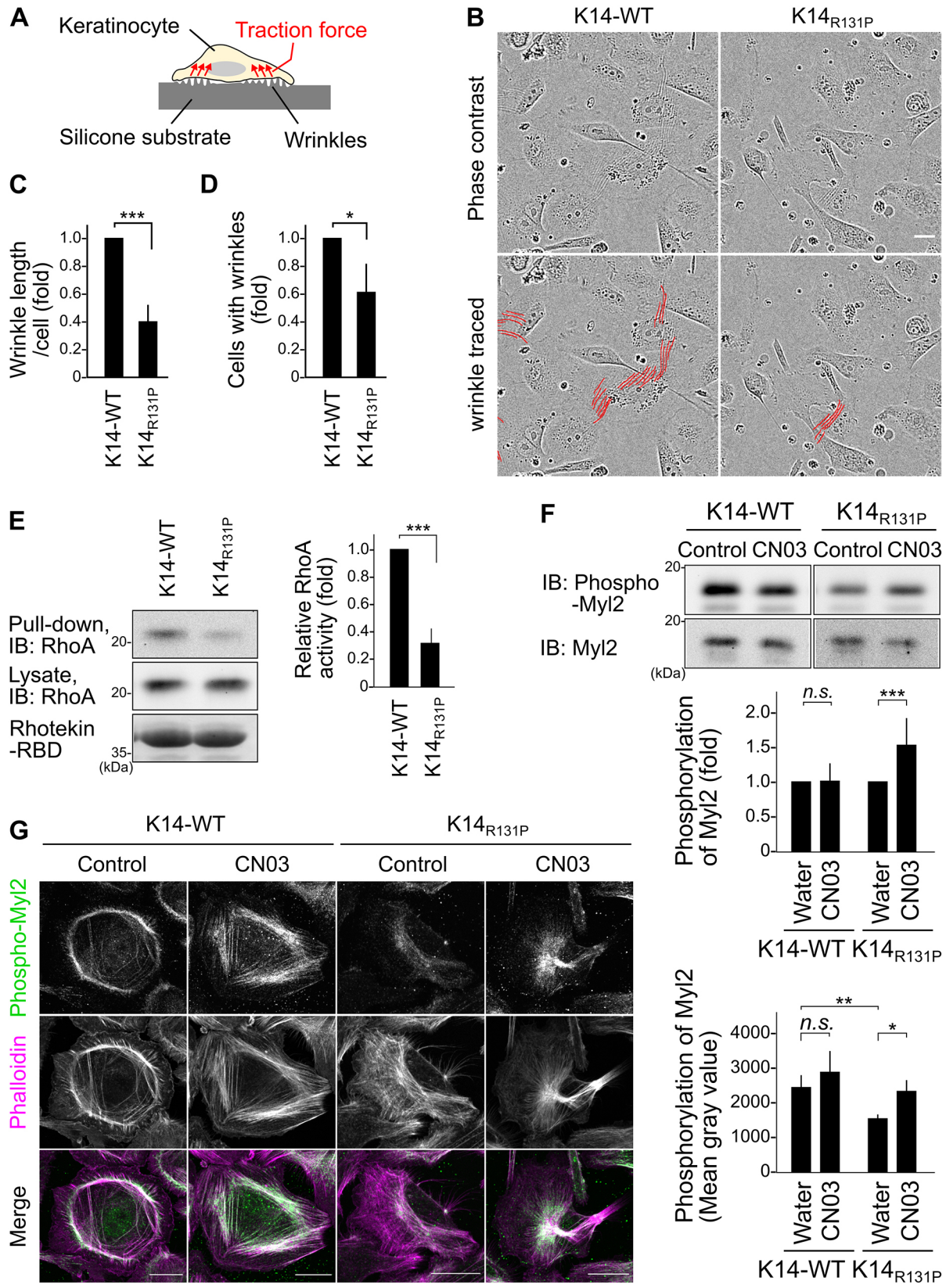

Fig. 1. Keratin organization affects traction force generation and RhoA activities. (A) Schematic illustration of cells cultured on a silicone substrate. (B) Wrinkle formation assay. Lower panels show the overlaid images of the wrinkles (red lines). Scale bar: 20 µm. (C,D) Quantification of traction force generation of keratinocytes. Wrinkle length per cell (C) and the number of cells forming wrinkles (D) were calculated from at least 11 images with on average 87 cells in each image. (E) RhoA activity analyzed by pulldown assays. Active RhoA was pulled down using the Rho-binding domain (RBD) of rhotekin. IB, immunoblot. (F) Levels of phosphorylated and total Myl2. (G) Immunostaining of phospho-Myl2 and phalloidin staining of F-actin. Scale bars: 20 µm. (E–G) The data shown represent the mean±s.d. of at least three independent experiments. *P<0.05, **P<0.01, ***P<0.001, n.s., not significant.

Journal of Cell Science (2020) 133, jcs243956. doi:10.1242/jcs.243956

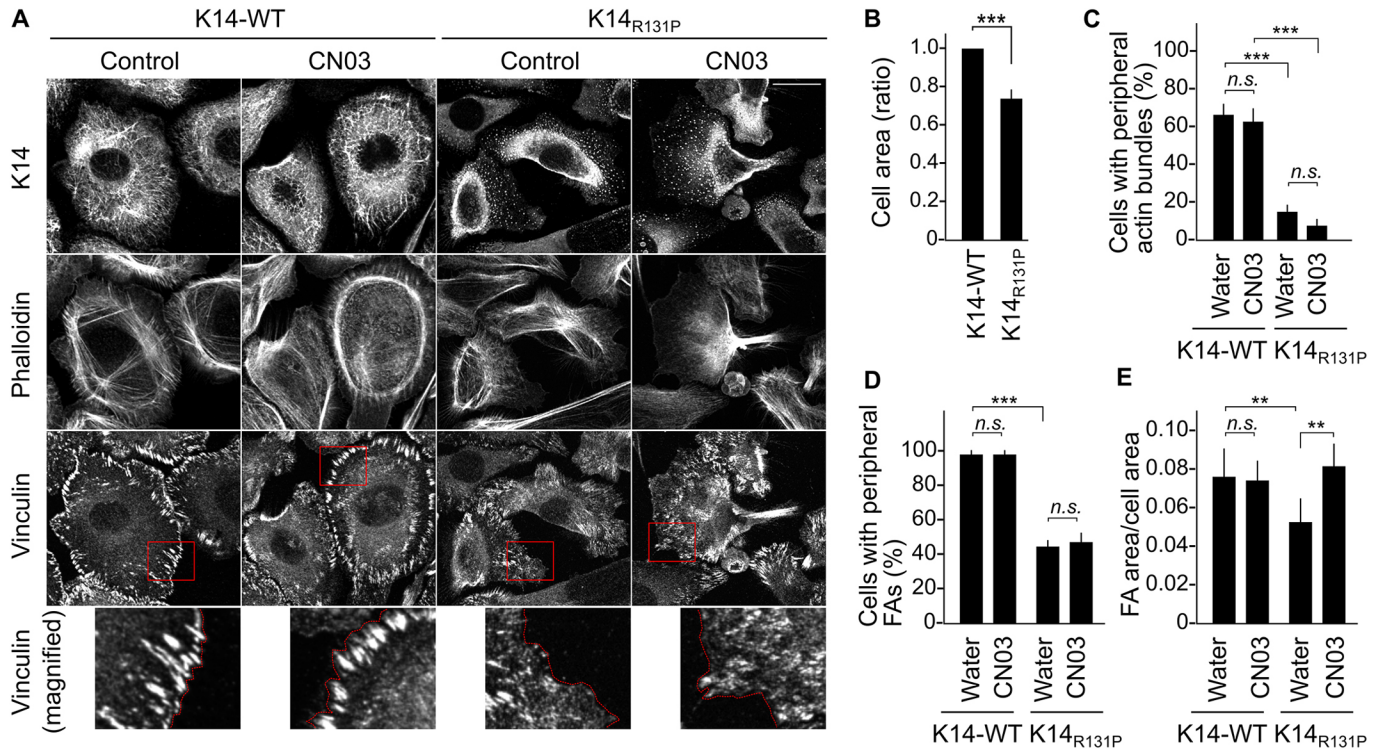

Fig. 2. Keratin organization affects cell morphology, actin reorganization, and focal adhesion distribution through Rho signaling pathways. (A) Fluorescence images of K14, F-actin (phalloidin), and vinculin. Magnified images of the regions indicated by red boxes are shown in the bottom panels. The dotted red lines mark the cell outlines. Note that peripheral vinculin signals are missing in $K14_{R131P}$ cells. Scale bar: 20 µm. (B) Cell area, normalized to K14-WT area. (C) Percentage of cells with peripheral actin bundles. (D) Percentage of cells with FAs at the cell peripheral regions, calculated based on the immunostaining images of vinculin. (E) Proportion of total FA area in a cell area. (B–E) The data shown represent the mean±s.d. of three independent experiments (at least 60 cells per experiment). $^{**}P<0.01$, $^{***}P<0.001$, n.s., not significant.

adhesion, formation and localization of $K14_{R131P}$ aggregates is independent of plectin.

Intact keratin IF networks and the activity of Rho and YAP are important for substrate stiffness-dependent cell adhesion formation

Matrix stiffness controls proliferation, survival and migration (Engler et al., 2006; Yeh et al., 2017; Martino et al., 2018). To further elucidate the involvement of keratin organization in mechanotransduction, we examined cell adhesion formation on soft collagen substrates (Fig. 3A,B). K14-WT attached and spread in a single layer on a gel, similar to the morphology observed on a collagen-coated glass surface, whereas the percentage of $K14_{R131P}$ that attached and spread on a gel was significantly decreased (Fig. 3B–D, Water). In addition, K14-WT showed vinculin signals enriched at the cell periphery, whereas in $K14_{R131P}$, vinculin lacked an obvious enrichment at the plasma membrane (Fig. 3B, Water). To examine the involvement of Rho signaling in keratin-mediated cell adhesion on a soft substrate, endogenous Rho activity was restored using CN03 treatment. Treatment of $K14_{R131P}$ with CN03 significantly increased the percentage of spread cells with peripheral FAs (Fig. 3D,E).

To substantiate the involvement of keratins in mechanotransduction, we turned to YAP/TAZ (also known as YAP1 and WWTR1, respectively), which are important regulators of cell–matrix adhesion-mediated signaling by acting as mechanosensing switches. Stiffness-dependent cell spreading is associated with YAP/TAZ nuclear translocation to exert their co-transcriptional activity (Dupont et al., 2011; Nardone et al., 2017; Wang et al., 2020). Immunofluorescence analysis revealed that YAP mainly localized in the nucleus of K14-WT, whereas it remained in the cytoplasm of $K14_{R131P}$ (Fig. 3F,G). Considering that cells actively sense the rigidity of the surrounding ECM by exerting traction forces to determine cell functions, including adhesion formation (Chen et al., 2015; Jansen et al., 2015), our results raise the possibility that an intact keratin network contributes to substrate stiffness sensing and peripheral FA formation, involving Rho signaling.

Disorganization of keratins leads to downregulation and mislocalization of FAK

FAK (also known as PTK2) is a key regulator of FAs. Because size and distribution of FAs were different between K14-WT and $K14_{R131P}$, we focused on FAK signaling. The Y397 of FAK is the main site of autophosphorylation induced by integrin binding to the ECM. Phosphorylation of Y397 generates an SH2 binding site for Src family kinases and induces phosphorylation of other residues, including Y925 (Westhoff et al., 2004; Deramaudt et al., 2011). Analysis of FAK phosphorylation showed lower phosphorylation levels of FAK-Y925 in $K14_{R131P}$ compared to control cells, whereas FAK-Y397 remained unaltered (Fig. 4A–C). Analysis of Src, which phosphorylates FAK-Y925 (Brunton et al., 2005), revealed significantly lower levels in $K14_{R131P}$ compared to levels in K14-WT (Fig. 4D,E). To substantiate the involvement of Src, we used the inhibitor PP1 to block Src phosphorylation and activation. PP1 indeed inhibited Src phosphorylation and significantly decreased FAK-Y925 phosphorylation levels (Fig. 4F–H). Thus, an intact keratin network is required for Src activation and Src-mediated

Journal of Cell Science (2020) 133, jcs243956. doi:10.1242/jcs.243956

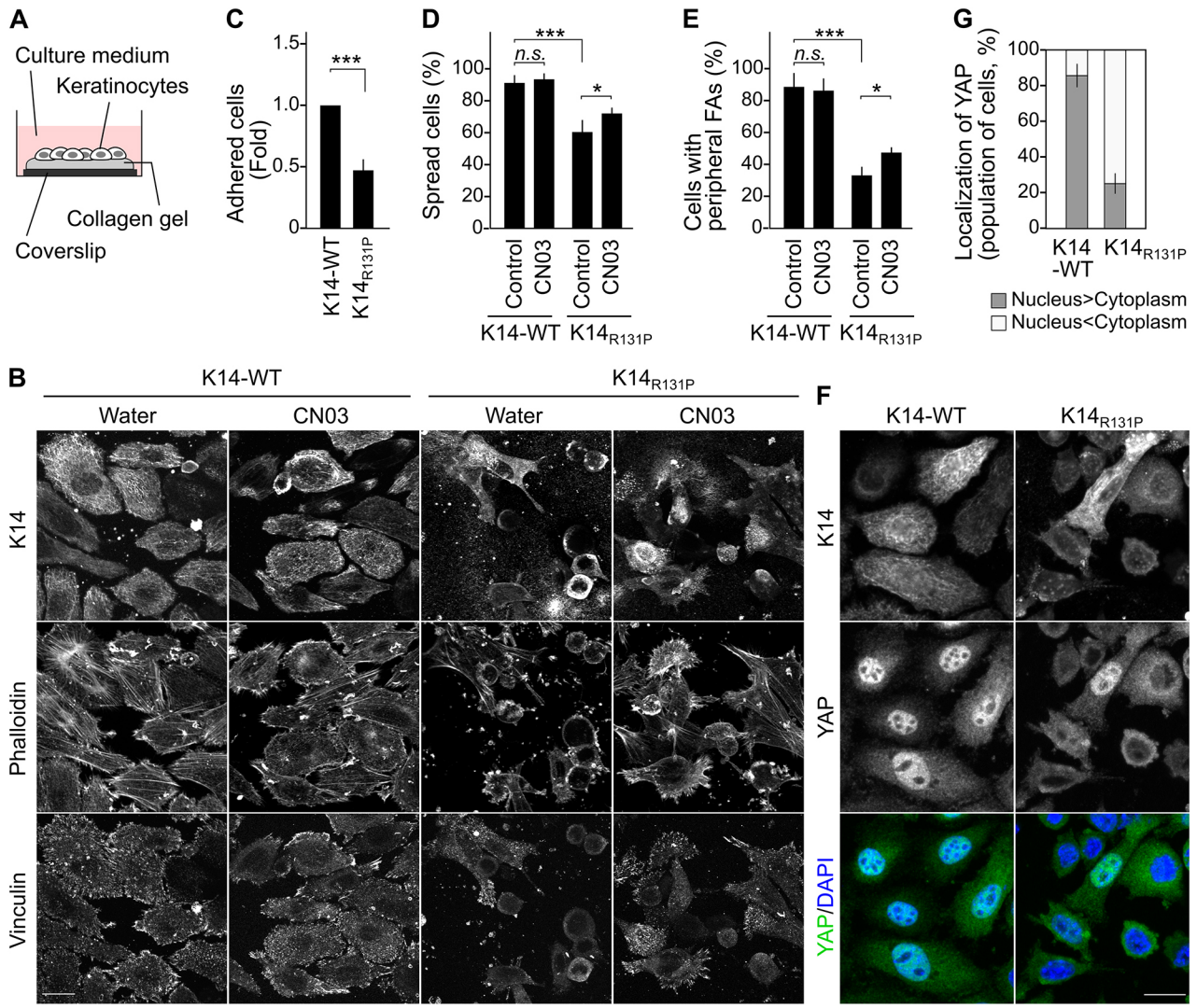

Fig. 3. Keratin organization affects cell spreading and migration ability on a soft substrate through Rho signaling and YAP. (A) Schematic illustration of cells cultured on a collagen gel. (B) Fluorescence images of K14, F-actin (phalloidin), and vinculin in cells on a gel. Scale bar: 20 µm. (C–E) Percentage of cells attached on a gel (C, normalized to K14-WT), spread on a gel (D) and with peripheral FAs (E). (F) Fluorescence images of K14 and YAP, with DNA stained using DAPI. Scale bar: 20 µm. (G) Quantification of the nuclear localization of YAP. (C–E,G) The data shown represent the mean±s.d. of three independent experiments [at least 63 cells (C–E) and 26 cells (G) per experiment]. **P*<0.05, ****P*<0.001, n.s., not significant.

phosphorylation of FAK-Y925. To correlate FAK activity to the state of FA, we monitored its localization. Although FAK localized along the entire basal surface and concentrated at the cell periphery in K14-WT, the peripheral localization was not obvious in $K14_{R131P}$ (Fig. 4I,J). This suggests that the $K14_{R131P}$ mutation affects focal adhesion formation, accompanied by altered localization and activation of FAK.

Keratin aggregates reduce directionality during collective cell migration

Keratinocytes often collectively migrate during fundamental biological processes, such as wound healing and morphogenesis. The dynamics of collective migration are determined by the force balance between protrusive and adhesive forces (Trepat et al., 2009; George et al., 2017). IFs are involved in collective cell migration by regulating cell adhesion. For example, knockdown of GFAP, vimentin, and nestin restricts collective migration of astrocytes by compromising dynamics of adherens junctions and FAs (de Pascalis et al., 2018), and knockout of K6 in keratinocytes disrupts desmosomal adhesion and increases FA turnover, which accelerates collective migration (Wang et al., 2018). We investigated the impact of keratin network disruption on collective migration in a wound healing assay (Fig. S1A). Time-lapse imaging showed that leader cells appeared and migrated in both K14-WT and $K14_{R131P}$ collectives (Fig. S1B; Movies 1, 2). Whereas leader cells in K14-WT group migrated along relatively straight tracks oriented almost vertically to the wound edge, $K14_{R131P}$ leaders showed little directionality during migration (Fig. S1B,D), and the directional persistence was significantly lower than that of K14-WT (Fig. S1C,F). The average migration velocity of $K14_{R131P}$ was significantly faster than that of K14-WT (Fig. S1E). These results suggest that the migration velocity and the coordinated movement of cell groups depends on an intact keratin network. The activity of Rho GTPases plays a crucial role in directed collective migration by regulating protrusions and retractions through cytoskeletal reorganization (Lawson and Ridley, 2018). Impaired directed collective migration and reduced RhoA activity in $K14_{R131P}$ is consistent with defects in directed migration in RhoA-null keratinocytes (Fig. 1E; Jackson et al.,

Journal of Cell Science (2020) 133, jcs243956. doi:10.1242/jcs.243956

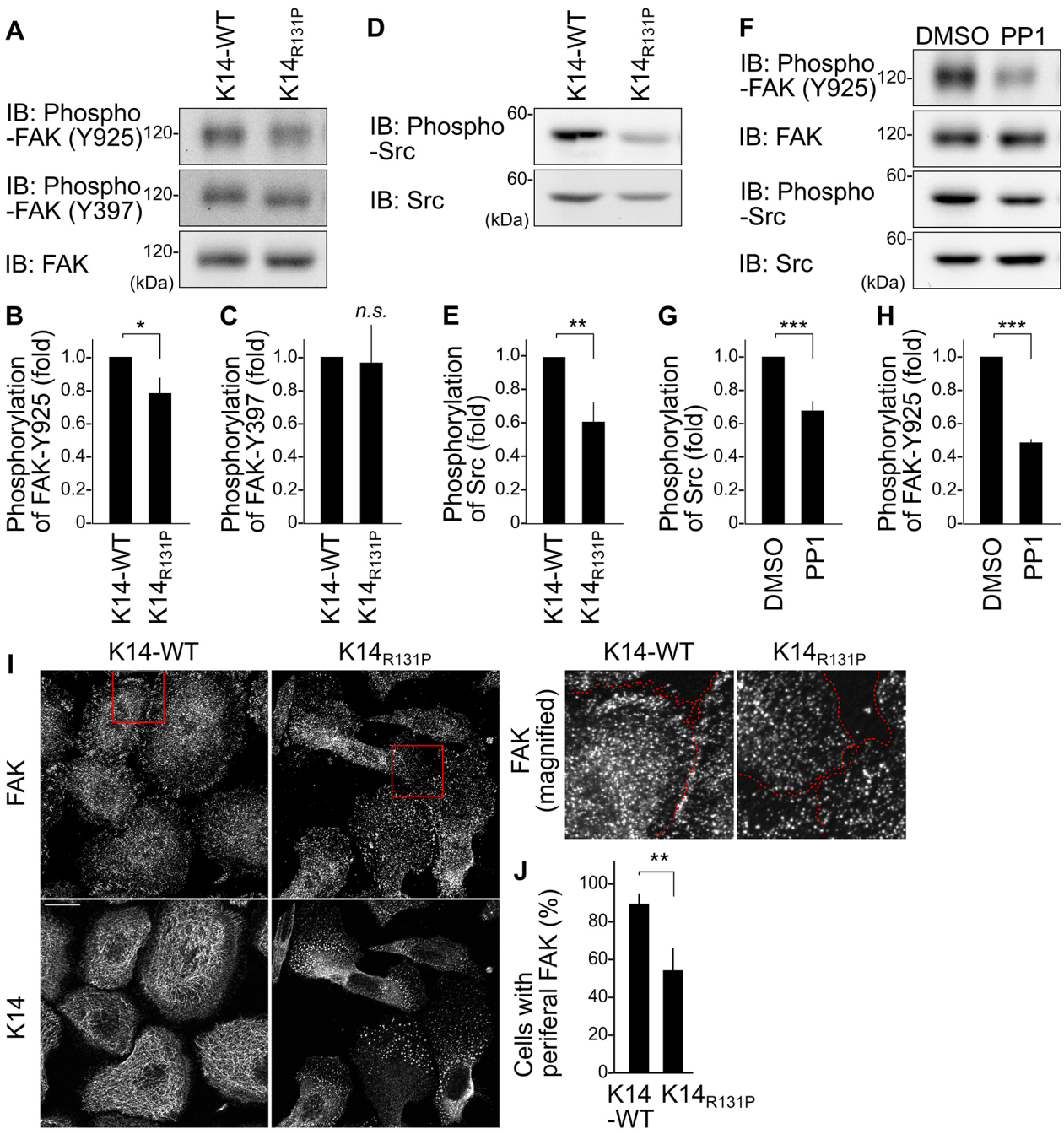

Fig. 4. Disorganized keratin leads to downregulation of FAK through the Src pathway. (A–E) Phosphorylation and total protein levels of FAK and Src. IB, immunoblot. (F–H) Effects of treatment with the Src inhibitor PP1 on the phosphorylation levels of FAK (G) and Src (H), relative to DMSO vehicle control. (I) Fluorescence images of K14 and FAK. Magnified images of the regions indicated by red boxes are shown to the right. Dotted lines show the cell outlines. Scale bar: 20 µm. (J) Percentage of cells with FAK signals at the cell peripheral regions. (A–H,J) The data shown represent the mean±s.d. of at least three independent experiments. *P<0.05, **P<0.01, ***P<0.001, n.s., not significant.

2011). This suggests that disturbed migration results from defective RhoA activation, in addition to weakened desmosome adhesion in $K14_{R131P}$ (Homberg et al., 2015).

It remains unknown how keratins contribute to the regulation of RhoA signaling. p190RhoGEF (also known as ARHGEF28) interacts with FAK and is activated by mechanotransduction (Zhai et al., 2003). The interaction of Solo (also known as ARHGEF40) with keratin 18 is important for tensional force-induced RhoA activation and traction force generation (Fujiwara et al., 2016, 2019). We hypothesize that keratin networks participate in regulation of RhoA by affecting activities and/or localization of RhoGEFs such as p190RhoGEF and Solo, contributing to traction force generation through actin reorganization and FA formation. Activation of FAs can further activate RhoA, thus traction force generation drives a positive feedback loop. Considering that FA formation is downregulated in $K14_{R131P}$, unlike in keratin knockout cells, aggregated keratins possibly inhibit RhoA activation, resulting in force imbalance. Our observations suggest that defects in force sensing and mechanotransduction associated with keratin mutations contribute to EBS.

Journal of Cell Science (2020) 133, jcs243956. doi:10.1242/jcs.243956

MATERIALS AND METHODS

Reagents and antibodies

Type I collagen (354236) was purchased from Corning (Corning, NY). Rho activator II (CN03) was purchased from Cytoskeleton (Denver, CO) and used at 4 µg/ml for 4 h. PP1 was purchased from Biomol (Hamburg, Germany) and used at 10 µM for 1 h. Alexa Fluor®-647-labeled phalloidin (A22287) was purchased from Thermo Fisher Scientific (Waltham, MA). An antibody against plectin is from Dr H. Herrmann [Division of Cell Biology, German Cancer Research Center (DKFZ), 69120 Heidelberg, Germany]. Other antibodies were purchased as follows: anti-keratin14 (ab181595, Abcam, Cambridge, UK), anti-vinculin (V9131, Sigma Aldrich, St Louis, MO), anti-RhoA (sc-418, Santa Cruz Biotechnology, Dallas, TX), anti-GAPDH (sc-25778, Santa Cruz Biotechnology or G7895, Sigma Aldrich), anti-YAP (sc101199, Santa Cruz Biotechnology), anti-phospho FAK (Tyr397) (3283S, Cell Signaling Technology, Danvers, MA), anti-phospho FAK (Tyr925) (3284S, Cell Signaling Technology), anti-FAK (3285S, Cell Signaling Technology), anti-phospho Src (Tyr416) (6943S, Cell Signaling Technology), anti-Src (2108S, Cell Signaling Technology), anti-phospho-Myl2 (Thr18/Ser19) (3674S, Cell Signaling Technology) and anti-Myl2 (3672S, Cell Signaling Technology). Secondary antibodies used for immunoblotting and immunofluorescence analysis were purchased from Dianova (Hamburg, Germany).

siRNA transfection

The siRNA targeting the murine sequence of plectin was purchased from siTOOLs Biotech (Munich, Germany). siRNA was transfected using Lipofectamine® RNAiMAX (Life Technologies). The siRNAs were used at a final concentration of 30 nM. Transfected cells were cultured for 48 h before being subjected to experiments. Knockdown efficiency of plectin1 mRNA expression was analyzed by reverse transcription PCR followed by quantitative PCR analysis using specific primers (plectin1 forward, 5′-CCCAGGATGAGAAGGAACAAC-3′; plectin1 reverse; 5′-GCACAAGAAAGCACACAGAAG-3′; GAPDH forward, 5′-GTGTTCCTACCCCCAATGTG-3′; GAPDH reverse, 5′-AGGAGACAACCTGGTCCTCA-3′).

Cell culture

Mouse keratinocytes were established and cultured as described previously (Kröger et al., 2013; Ramms et al., 2013; Homberg et al., 2015). For culturing cells on a plastic, a glass, or a silicone substrate, the surface was coated with 5 µg/cm^2 type I collagen. To prepare a type I collagen gel for analyzing cells cultured on a soft substrate, a collagen solution was neutralized by adding NaOH, $NaHCO_3$, and 10× PBS, and the concentration was adjusted to 3% with culture medium consequently to have an elastic modulus of 50–100 Pa (Valero et al., 2018; and according to the application notes of the manufacturer) and spread on 13-mm coverslips placed in a 24-well culture plate. After fabrication of the collagen by placing the plate at 37°C for at least 20 min, cells were seeded in the well and cultured for 48 h. Normal human keratinocytes (NHK) and $K14_{R131C}$ cells were kindly provided by Prof. Dr C. Has (Uniklinik Freiburg, Freiburg im Breisgau, Germany) and cultured in keratinocyte serum-free medium supplemented with L-glutamine, EGF and BPE (#17005-075, Thermo Fisher Scientific).

GST–RBD pulldown assay

The active form of RhoA was detected by pulldown assays using the Rho-binding domain (RBD) of rhotekin fused to GST, as described previously (Ren and Schwartz, 2000). Cells were cultured for 48–72 h in growth medium, and cell lysates were subjected to pulldown assays.

Immunoblot analysis

Total cell lysates were subjected to analysis of protein phosphorylation and protein expression analysis. Protein phosphorylation levels were calculated by correcting for the total amount of the proteins. Immunoblotting was performed under the following conditions: blocking with 5% skim milk in TBS-T (Tris-buffered saline containing 0.1% Tween® 20) for 40 min at room temperature; primary antibody incubation in TBS-T containing 5% BSA overnight at 4°C; secondary antibody incubation in TBS-T containing 5% skim milk for 50 min at room temperature. Primary antibodies were used at the following dilutions: anti-keratin 14, 1:50,000; anti-vinculin, 1:1000; anti-RhoA, 1:60; anti-GAPDH, 1:2000; anti-phospho FAK (Tyr397), 1:2000; anti-phospho FAK (Tyr925), 1:2000; anti-FAK, 1:2000; anti-phospho Src, 1:2000; anti-Src, 1:2000; anti-phospho Myl2, 1:2000; anti-Myl2, 1:1000; anti-plectin, 1:2000.

Immunofluorescence staining and fluorescence imaging

Cells cultured on type I collagen-coated coverslips and on 3% type I collagen gel were fixed with 2% (w/v) paraformaldehyde in phosphate-buffered saline (PBS) at room temperature for 20 min and then permeabilized with 0.1% Triton X-100™ in PBS for 3 min. Exceptions to this were that cells were fixed with 10% TCA on ice for 15 min for staining endogenous RhoA and with cold methanol at −20°C for 3 min for double staining of plectin and K14. Cells were treated with 5% BSA in TBS for blocking and were incubated with primary antibodies for 90 min and secondary antibodies for 40 min at room temperature. Primary antibodies were used at the following dilutions: anti-keratin 14, 1:600; anti-vinculin, 1:600; anti-RhoA, 1:50; anti-YAP, 1:200; anti-FAK, 1:400; anti-plectin, 1:400; anti-phospho-Myl2, 1:100. Fluorescence images were obtained using an LSM780 confocal microscope (Carl Zeiss) equipped with a PL-Apo 40× oil objective lens (NA 1.3) for mouse keratinocytes and a PL-Apo 63× oil objective lens (NA 1.46) for human keratinocytes. Image quantifications of FAs in each cell were performed using ImageJ software (National Institutes of Health). We used maximum intensity projection images of 0.5 µm from the ventral surface for the analysis. Images were processed with the 'Subtract Background' command, and the 'Threshold' command was run to convert images to binary images before executing the 'Analyze Particles' command (particle size, >0.1 µm^2). The region of interest (ROI) was set to the outline of each cell. To calculate the proportion of total FA area in a cell area, total FA area of each cell was divided by the cell area measured by tracing the outline of each cell.

Wrinkle formation assay

Cell traction force was visualized using a wrinkle-generating method as described previously (Ichikawa et al., 2017), except that the silicone substrates CY 52-276 were mixed at a weight ratio of 1.2:1 and spread on coverslips. The coverslip was put on a 6-well culture plate and coated with type I collagen. Cells were seeded in a well at a density that enabled recognition of the circumference of each single cell after culturing for 48 h–72 h, and images in which the total area covered by the cells were the same were selected for image analysis. Phase-contrast images were obtained using an IncuCyte microscope (Sartorius, Göttingen, Germany) equipped with a 20× objective lens (NA 0.45) placed in a 5% CO_2 incubator. Cellular traction force generation was evaluated by manually tracing the wrinkles on the silicone surface surrounding the cell in the phase-contrast image, and the length of wrinkles was analyzed by using ImageJ software. The wrinkle length per cell was calculated by dividing the wrinkle length in a whole image by the number of cells in the image. The ratio of the mean total wrinkle length per cell of $K14_{R131P}$ to that of K14-WT was calculated in each experiment.

Time-lapse observation of collective migration

For observation of collective cell migration, keratinocytes were seeded in a rounded rectangle-shaped silicone well (growth area 0.22 cm^2, Ibidi) placed on a glass-bottomed dish coated with type I collagen in a low calcium medium (0.05 mM $CaCl_2$) and incubated overnight. Then the culture media were replaced with a high calcium medium (2 mM $CaCl_2$) and incubated for an additional 24 h, and the silicone well was removed. After culture for 5 h in the high calcium medium, cells were subjected to a time-lapse analysis using a spinning disc confocal microscope (Carl Zeiss) equipped with a 10×/0.3 EC Plan-Neofluar objective lens. During image acquisition, the dish was placed in a CO_2 chamber set on the stage of the microscope, and the microscope was covered with a temperature hood to maintain the stage temperature at 32°C. Phase-contrast images were acquired every 15 min for at least 5 h. Nuclei of leader cells that did not detach from the cell group during 5 h time-lapse imaging were tracked using the manual tracking tool in ImageJ. The coordinate of each cell was calculated by correcting the angle of the wound edge as 0° and the start position as: (X_0, X_0)=(0,0), and the

parameters for 5 h of migration were calculated with the following formulae, where (X_n, Y_n) indicates the coordinate of a cell at the timepoint n (min). Distance (μm): $d = \sum \sqrt{(X_{300} - X_0)^2 + (Y_{300} - Y_0)^2}$. Total travel distance (μm): $d_{total} = \sum \sqrt{(X_n - X_{n-1})^2 + (Y_n - Y_{n-1})^2}$. Mean velocity (μm/min): $v = d_{total}/300$. Directional persistence: $p = d/d_{total}$.

Statistical analysis

Data are expressed as the mean±s.d. of more than three independent experiments. Statistical analysis was performed using Prism 8 (Graphpad Software, La Jolla, CA). *P*-values were calculated using a one-way analysis of variance (ANOVA) followed by Tukey's test or a two-tailed paired *t*-test. The threshold for statistical significance was set at $P<0.05$.

Acknowledgements

We thank T. S. Matsui (Osaka University, Japan) for his help and support with wrinkle formation assay and C. Has (Uniklinik Freiburg, Germany) for providing $K14_{R125C}$.

Competing interests

The authors declare no competing or financial interests.

Author contributions

Conceptualization: S.F.; Methodology: S.F., S.D.; Validation: S.F.; Formal analysis: S.F., S.D.; Investigation: S.F.; Resources: S.F., S.D.; Data curation: S.F.; Writing - original draft: S.F.; Writing - review & editing: S.F., T.M.M.; Visualization: S.F.; Supervision: S.F., T.M.M.; Project administration: S.F., T.M.M.; Funding acquisition: S.F., S.D., T.M.M.

Funding

S.F. was supported by a Uehara Memorial Foundation Research Fellowship. This work was supported by funding from Ministry of Education, Culture, Sports, Science and Technology (MEXT) KAKENHI grant no. 15H03004 to S.D., and Deutsche Forschungsgemeinschaft (DFG) grants no. MA1316/19-1 and MA1316/21-2 to T.M.M. The BioImaging Core Facility of University of Leipzig is supported by INST268/230-1 to T.M.M.

Supplementary information

Supplementary information available online at
https://jcs.biologists.org/lookup/doi/10.1242/jcs.243956.supplemental

Peer review history

The peer review history is available online at
https://jcs.biologists.org/lookup/doi/10.1242/jcs.243956.reviewer-comments.pdf

References

Block, J., Schroeder, V., Pawelzyk, P., Willenbacher, N. and Köster, S. (2015). Physical properties of cytoplasmic intermediate filaments. *Biochim. Biophys. Acta Mol. Cell Res.* **1853**, 3053-3064. doi:10.1016/j.bbamcr.2015.05.009

Brunton, V. G., Avizienyte, E., Fincham, V. J., Serrels, B., Metcalf, C. A., Sawyer, T. K. and Frame, M. C. (2005). Identification of Src-specific phosphorylation site on focal adhesion kinase: dissection of the role of Src SH2 and catalytic functions and their consequences for tumor cell behavior. *Cancer Res.* **65**, 1335-1342. doi:10.1158/0008-5472.CAN-04-1949

Chrzanowska-Wodnicka, M. and Burridge, K. (1996). Rho-stimulated contractility drives the formation of stress fibers and focal adhesions. *J. Cell Biol.* **133**, 1403-1415. doi:10.1083/jcb.133.6.1403

Coulombe, P. A. and Lee, C.-H. (2012). Defining keratin protein function in skin epithelia: epidermolysis bullosa simplex and its aftermath. *J. Invest. Dermatol.* **132**, 763-775. doi:10.1038/jid.2011.450

Chen, B., Ji, B. and Gao, H. (2015). Modeling active mechanosensing in cell-matrix Interactions. *Ann. Rev. Biophys.* **44**, 1-32. doi:10.1146/annurev-biophys-051013-023102

D'Alessandro, M., Russell, D., Morley, S. M., Davies, A. M. and Lane, E. B. (2002). Keratin mutations of epidermolysis bullosa simplex alter the kinetics of stress response to osmotic shock. *J. Cell Sci.* **115**, 4341-4351. doi:10.1242/jcs.00120

De Pascalis, C., Pérez-González, C. P., Seetharaman, S., Boëda, B., Vianay, B., Burute, M., Leduc, C., Borghi, N., Trepat, X. and Etienne-Manneville, S. (2018). Intermediate filaments control collective migration by restricting traction forces and sustaining cell – cell contacts. *J. Cell Biol.* **217**, 3031-3044. doi:10.1083/jcb.201801162

Deramaudt, T. B., Dujardin, D., Hamadi, A., Noulet, F., Kolli, K., De Mey, J., Takeda, K. and Rondé, P. (2011). FAK phosphorylation at Tyr-925 regulates cross-talk between focal adhesion turnover and cell protrusion. *Mol. Biol. Cell* **22**, 964-975. doi:10.1091/mbc.e10-08-0725

Dufort, C. C., Paszek, M. J. and Weaver, V. M. (2011). Balancing forces: architectural control of mechanotransduction. *Nat. Rev. Mol. Cell Biol.* **12**, 308-319. doi:10.1038/nrm3112

Dupont, S., Morsut, L., Dupont, S., Morsut, L., Aragona, M., Enzo, E., Giulitti, S., Cordenonsi, M., Zanconato, F., Le Digabel, J. et al. (2011). Role of YAP/TAZ in mechanotransduction. *Nature* **474**, 179-183. doi:10.1038/nature10137

Engler, A. J., Sen, S., Sweeney, H. L. and Discher, D. E. (2006). Matrix elasticity directs stem cell lineage specification. *Cell* **126**, 677-689. doi:10.1016/j.cell.2006.06.044

Etienne-Manneville, S. (2018). Cytoplasmic intermediate filaments in cell biology. *Annu. Rev. Cell Dev. Biol.* **34**, 1-28. doi:10.1146/annurev-cellbio-100617-062534

Evans, N. D., Oreffo, R. O. C., Healy, E., Thurner, P. J. and Man, Y. H. (2013). Epithelial mechanobiology, skin wound healing, and the stem cell niche. *J. Mech. Behav. Biomed. Mater.* **28**, 397-409. doi:10.1016/j.jmbbm.2013.04.023

Eyckmans, J., Boudou, T., Yu, X. and Chen, C. S. (2011). A Hitchhiker's guide to mechanobiology. *Dev. Cell* **21**, 35-47. doi:10.1016/j.devcel.2011.06.015

Fujiwara, S., Ohashi, K., Mashiko, T., Kondo, H. and Mizuno, K. (2016). Interplay between Solo and keratin filaments is crucial for mechanical forceinduced stress fiber reinforcement. *Mol. Biol. Cell* **27**, 954-966. doi:10.1091/mbc.E15-06-0417

Fujiwara, S., Matsui, T. S., Ohashi, K., Mizuno, K. and Deguchi, S. (2019). Keratin-binding ability of the N-terminal Solo domain of Solo is critical for its function in cellular mechanotransduction. *Genes Cells* **24**, 390-402. doi:10.1111/gtc.12682

George, M., Bullo, F. and Campàs, O. (2017). Connecting individual to collective cell migration. *Sci. Rep.* **7**, 9720. doi:10.1038/s41598-017-10069-8

Gilbert, S., Loranger, A., Daigle, N. and Marceau, N. (2001). Simple epithelium keratins 8 and 18 provide resistance to Fas-mediated apoptosis. The protection occurs through a receptor-targeting modulation. *J. Cell Biol.* **154**, 763-773. doi:10.1083/jcb.200102130

Hatzfeld, M., Keil, R. and Magin, T. M. (2017). Desmosomes and intermediate filaments: their consequences for tissue mechanics. *Cold Spring Harb. Perspect. Biol.* **9**, a029157. doi:10.1101/cshperspect.a029157

Homberg, M. and Magin, T. M. (2014). Beyond expectations: novel insights into epidermal keratin function and regulation. *Int. Rev. Cell Mol. Biol.* **311**, 265-306. doi:10.1016/B978-0-12-800179-0.00007-6

Homberg, M., Ramms, L., Schwarz, N., Dreissen, G., Leube, R. E., Merkel, R., Hoffmann, B. and Magin, T. M. (2015). Distinct impact of two keratin mutations causing epidermolysis bullosa simplex on keratinocyte adhesion and stiffness. *J. Invest. Dermatol.* **135**, 2437-2445. doi:10.1038/jid.2015.184

Hsu, C.-K., Lin, H.-H., Harn, H. I.-C., Hughes, M. W., Tang, M.-J. and Yang, C.-C. (2018). Mechanical forces in skin disorders. *J. Dermatol. Sci.* **90**, 232-240. doi:10.1016/j.jdermsci.2018.03.004

Ichikawa, T., Kita, M., Matsui, T. S., Nagasato, A. I., Araki, T., Chiang, S.-H., Sezaki, T., Kimura, Y., Ueda, K., Deguchi, S. et al. (2017). Vinexin family (SORBS) proteins play different roles in stiffness-sensing and contractile force generation. *J. Cell Sci.* **130**, 3517-3531. doi:10.1242/jcs.200691

Inada, H., Izawa, I., Nishizawa, M., Fujita, E., Kiyono, T., Takahashi, T., Momoi, T. and Inagaki, M. (2001). Keratin attenuates tumor necrosis factor-induced cytotoxicity through association with TRADD. *J. Cell Biol.* **155**, 415-426. doi:10.1083/jcb.200103078

Ishizaki, T., Naito, M., Fujisawa, K., Maekawa, M., Watanabe, N., Saito, Y. and Narumiya, S. (1997). $p160^{ROCK}$, a Rho-associated coiled-coil forming protein kinase, works downstream of Rho and induces focal adhesions. *FEBS Lett.* **404**, 118-124. doi:10.1016/S0014-5793(97)00107-5

Iskratsch, T., Wolfenson, H. and Sheetz, M. P. (2014). Appreciating force and shape-the rise of mechanotransduction in cell biology. *Nat. Rev. Mol. Cell Biol.* **15**, 825-833. doi:10.1038/nrm3903

Jackson, B., Peyrollier, K., Pedersen, E., Basse, A., Karlsson, R., Wang, Z., Lefever, T., Ochsenbein, A. M., Schmidt, G., Aktories, K. et al. (2011). RhoA is dispensable for skin development, but crucial for contraction and directed migration of keratinocytes. *Mol. Biol. Cell* **22**, 593-605. doi:10.1091/mbc.e09-10-0859

Jaffe, A. B. and Hall, A. (2005). RHO GTPASES: biochemistry and biology. *Annu. Rev. Cell Dev. Biol.* **21**, 247-269. doi:10.1146/annurev.cellbio.21.020604.150721

Jansen, K. A., Donato, D. M., Balcioglu, H. E., Schmidt, T., Danen, E. H. J. and Koenderink, G. H. (2015). A guide to mechanobiology: Where biology and physics meet. *Biochim. Biophys. Acta* **1853**, 3043-3052. doi:10.1016/j.bbamcr.2015.05.007

Jiu, Y., Lehtimäki, J., Tojkander, S., Cheng, F., Jäälinoja, H., Liu, X., Varjosalo, M., Eriksson, J. E. and Lappalainen, P. (2015). Bidirectional interplay between vimentin intermediate filaments and contractile actin stress fibers. *Cell Rep.* **11**, 1511-1518. doi:10.1016/j.celrep.2015.05.008

Jiu, Y., Peränen, J., Schaible, N., Cheng, F., Eriksson, J. E., Krishnan, R. and Lappalainen, P. (2017). Vimentin intermediate filaments control actin stress fiber assembly through GEF-H1 and RhoA. *J. Cell Sci.* **130**, 892-902. doi:10.1242/jcs.196881

Kranenburg, O., Poland, M., Gebbink, M., Oomen, L. and Moolenaar, W. H. (1997). Dissociation of LPA-induced cytoskeletal contraction from stress fiber formation by differential localization of RhoA. *J. Cell Sci.* **110**, 2417-2427.

Kröger, C., Loschke, F., Schwarz, N., Windoffer, R., Leube, R. E. and Magin, T. M. (2013). Keratins control intercellular adhesion involving PKC-α-mediated desmoplakin phosphorylation. *J. Cell Biol.* **201**, 681-692. doi:10.1083/jcb.201208162

Lawson, C. D. and Ridley, A. J. (2018). Rho GTPase signaling complexes in cell migration and invasion. *J. Cell Biol.* **217**, 447-457. doi:10.1083/jcb.201612069

Loschke, F., Seltmann, K., Bouameur, J.-E. and Magin, T. M. (2015). Regulation of keratin network organization. *Curr. Opin. Cell Biol.* **32**, 56-64. doi:10.1016/j.ceb.2014.12.006

Mariani, R. A., Paranjpe, S., Dobrowolski, R. and Weber, G. F. (2020). 14-3-3 targets keratin intermediate filaments to mechanically sensitive cell-cell contacts. *Mol. Biol. Cell. Mol Biol Cell* **31**, 930-943. doi:10.1091/mbc.E18-06-0373

Martino, F., Perestrelo, A. R., Vinarský, V., Pagliari, S. and Forte, G. (2018). Cellular mechanotransduction: from tension to function. *Front. Physiol.* **9**, 824. doi:10.3389/fphys.2018.00824

Michaelson, D., Silletti, J., Murphy, G., D'Eustachio, P., Rush, M. and Philips, M. R. (2001). Differential localization of Rho GTPases in live cells: Regulation by hypervariable regions and RhoGDI binding. *J. Cell Biol.*, **152**, 111-126. doi:10.1083/jcb.152.1.111

Nardone, G., Oliver-De La Cruz, J., Vrbsky, J., Martini, C., Pribyl, J., Skládal, P., Pešl, M., Caluori, G., Pagliari, S., Martino, F. et al. (2017). YAP regulates cell mechanics by controlling focal adhesion assembly. *Nat. Commun.* **8**, 15321. doi:10.1038/ncomms15321

Ramms, L., Fabris, G., Windoffer, R., Schwarz, N., Springer, R., Zhou, C., Lazar, J., Stiefel, S., Hersch, N., Schnakenberg, U. et al. (2013). Keratins as the main component for the mechanical integrity of keratinocytes. *Proc. Natl. Acad. Sci. USA* **110**, 18513-18518. doi:10.1073/pnas.1313491110

Ren, X.-D. and Schwartz, M. A. (2000). Determination of GTP loading on Rho. *Methods Enzymol.* **325**, 264-272. doi:10.1016/S0076-6879(00)25448-7

Rotty, J. D. and Coulombe, P. A. (2012). A wound-induced keratin inhibits Src activity during keratinocyte migration and tissue repair. *J. Cell Biol.* **197**, 381-389. doi:10.1083/jcb.201107078

Russell, D., Andrews, P. D., James, J. and Lane, E. B. (2004). Mechanical stress induces profound remodelling of keratin filaments and cell junctions in epidermolysis bullosa simplex keratinocytes. *J. Cell Sci.* **117**, 5233-5243. doi:10.1242/jcs.01407

Sanghvi-Shah, R. and Weber, G. F. (2017). Intermediate filaments at the junction of mechanotransduction, migration, and development. *Front. Cell Dev. Biol.* **5**, 81. doi:10.3389/fcell.2017.00081

Seltmann, K., Cheng, F., Wiche, G., Eriksson, J. E. and Magin, T. M. (2015). Keratins stabilize hemidesmosomes through regulation of β4-integrin turnover. *J. Invest. Dermatol.* **135**, 1609-1620. doi:10.1038/jid.2015.46

Snider, N. T. and Omary, M. B. (2014). Post-translational modifications of intermediate filament proteins: mechanisms and functions. *Nat. Rev. Mol. Cell Biol.* **15**, 163-177. doi:10.1038/nrm3753

Szeverenyi, I., Cassidy, A. J., Chung, C. W., Lee, B. T. K., Common, J. E. A., Ogg, S. C., Chen, H., Sim, S. Y., Goh, W. L. P., Ng, K. W. et al. (2008). The human intermediate filament database: comprehensive information on a gene family involved in many human diseases. *Hum. Mutat.* **29**, 351-360. doi:10.1002/humu.20652

Trepat, X., Wasserman, M. R., Angelini, T. E., Millet, E., Weitz, D. A., Butler, J. P. and Fredberg, J. J. (2009). Physical forces during collective cell migration. *Nat. Phys.* **5**, 426-430. doi:10.1038/nphys1269

Valero, C., Amaveda, H., Mora, M. and García-Aznar, J. M. (2018). Combined experimental and computational characterization of crosslinked collagen-based hydrogels. *PLoS ONE* **13**, e0195820. doi:10.1371/journal.pone.0195820

Wang, J., Zhang, Y., Zhang, N., Wang, C., Herrler, T. and Li, Q. (2015). An updated review of mechanotransduction in skin disorders: transcriptional regulators, ion channels, and microRNAs. *Cell. Mol. Life Sci.* **72**, 2091-2106. doi:10.1007/s00018-015-1853-y

Wang, F., Chen, S., Liu, H. B., Parent, C. A. and Coulombe, P. A. (2018). Keratin 6 regulates collective keratinocyte migration by altering cell–cell and cell–matrix adhesion. *J. Cell Biol.* **217**, 4314-4330. doi:10.1083/jcb.201712130

Wang, W., Zuidema, A., te Molder, L., Nahidiazar, L., Hoekman, L., Schmidt, T., Coppola, S. and Sonnenberg, A. (2020). Hemidesmosomes modulate force generation via focal adhesions. *J. Cell Biol.* **219**, e201904137. doi:10.1083/jcb.201904137

Westhoff, M. A., Serrels, B., Fincham, V. J., Frame, M. C. and Carragher, N. O. (2004). Src-mediated phosphorylation of focal adhesion kinase couples actin and adhesion dynamics to survival signaling. *Mol. Cell. Biol.* **24**, 8113-8133. doi:10.1128/MCB.24.18.8113-8133.2004

Wiche, G. (1998). Role of plectin in cytoskeleton organization and dynamics. *J. Cell Sci.* **1111**, 2477-2486.

Wong, P. and Coulombe, P. A. (2003). Loss of keratin 6 (K6) proteins reveals a function for intermediate filaments during wound repair. *J. Cell Biol.* **163**, 327-337. doi:10.1083/jcb.200305032

Yeh, Y.-C., Ling, J.-Y., Chen, W.-C., Lin, H.-H. and Tang, M.-J. (2017). Mechanotransduction of matrix stiffness in regulation of focal adhesion size and number: reciprocal regulation of caveolin-1 and β1 integrin. *Sci. Rep.* **7**, 15008. doi:10.1038/s41598-017-14932-6

Yonemura, S., Hirao-Minakuchi, K. and Nishimura, Y. (2004). Rho localization in cells and tissues. *Exp. Cell Res.*, **295**, 300-314. doi:10.1016/j.yexcr.2004.01.005

Zhai, J., Lin, H., Nie, Z., Wu, J., Cañete-Soler, R., Schlaepfer, W. W. and Schlaepfer, D. D. (2003). Direct interaction of focal adhesion kinase with p190RhoGEF. *J. Biol. Chem.* **278**, 24865-24873. doi:10.1074/jbc.M302381200